J Therm Anal Calorim (2011) 104:653–659
DOI 10.1007/s10973-010-0999-y

Chloro-free route to mixed-metal oxides. Synthesis of lead titanate nanoparticles from a single-source precursor route

Shidi Tang · Yuanfu Deng · ShuZhong Zhan

Received: 5 July 2010 / Accepted: 3 August 2010 / Published online: 18 August 2010

Abstract A new heterobimetallic nitrilotriacetatoperoxotitanate complex of titanium and lead $[Pb(H_2O)_3]_2[Ti_2(O_2)_2O(nta)_2]\cdot 4H_2O$ ($C_6H_6O_6N{=}H_3nta$) was isolated in pure crystals directly from the solution containing tetrabutyl orthotitanate, hydrogen peroxoide, lead acetate, and nitrilotriacetic acid at pH = 2.0–4.0. The isolated complex was characterized by elemental analyses, IR spectrum, thermal analysis (TG), and single-crystal X-ray diffraction. The single-crystal X-ray structural analysis revealed that the titanium atom is N,O,O′,O′′-chelated by the nitrilotriacetate and O,O′-chelated by the peroxo group and was coordinated to the bridging O atom in an overall pentagonal-bipyramidal geometry. The thermal decomposition of this precursor led to the formation of phase-pure lead titanate ($PbTiO_3$) at ≥450 °C. The morphology, microstructure, and crystalline of the resulting $PbTiO_3$ product have been characterized by BET, transmission electron microscopy, and powder X-ray diffraction. The TEM micrographs revealed that the size of the as-synthesized crystallines to be 50–100 nm range. The BET measurement revealed that the $PbTiO_3$ powders had a surface area of 5.6 m^2/g.

Keywords Single-source precursor · Lead titanate ($PbTiO_3$) · Nitrilotriacetatoperoxotitanate · Carboxylate-containing ligands

S. Tang · Y. Deng (✉) · S. Zhan
Department of Chemistry, School of Chemistry and Chemical Engineering, South China University of Technology, Guangzhou 510640, People's Republic of China
e-mail: chyfdeng@scut.edu.cn

Introduction

Over the last several decades, mixed-metal oxides incorporating lead and transition metals with a formula of ABO_3 have attracted broad interest due to their piezoelectricity, ferroelectricity, colossal magnetoresistivity, and photoluminescence [1–4]. However, the preparation of lead-containing mixed-metal oxides by traditional high-temperature solid state reaction is often difficult to control because of the volatility of PbO [5]. It has been shown both experimentally [6] and theoretically [7] that the properties of the mixed-metal oxides are strongly dependent on their composition, crystal morphology, surface area, and size. The functionality of mixed-metal oxides can be optimized by selecting suitable synthetic routes and, therefore, the scientific and technological importance of mixed-metal oxides continuously require the study and development of good synthetic approaches. Many soft chemistry methods, such as sol–gel [8], hydrothermal synthesis [9], and single-source precursor route [10], have provided general and affordable approaches for the preparation of mixed-metal oxides in various forms, with a continuous evolution of the material typologies, the exploited precursors, and the underlying chemistry.

The single-source precursor (SSPs) route, as one of the most promising approaches toward the preparation of the mixed-metal oxides, has received increasing attention because it provide lower temperature calcining process compared with the solid state or multi-source precursor approaches [11–21] and a much greater control of the metal stoichiometry in the final oxide compared with the sol–gel route [22]. In addition, the use of SSPs makes it possible to access new phases that are not available at higher reaction temperatures and thus provides more flexibility in the preparation of heterometallic oxide materials than conventional

methods [23]. However, one of the most significant challenges in developing the single-source precursor for the formation of mixed-metal oxide materials is the development of accessible synthetic approaches to obtain suitable precursors that allow to control over the stoichiometry of the individual metal species with relationship to one another in the final product. Up to now, some heterometallic lead-transition complexes have been explored as SSPs to mixed-metal oxides [23–28], however, to the best of our knowledge, few studies have been reported on the preparation of pure $PbTiO_3$ by structurally characterized SSPs because it is difficult to access to Pb–Ti species of 1:1 stoichiometry [10]. These precursors still have some disadvantages that they are handled only in a glove-box or Schlenk tube. In an effort to develop novel single-source precursors for mixed-metal oxides, we have been investigating the synthesis of air-stable carboxylate-based heterobimetallic coordination complexes from an environmentally benign point of view [29–37]. In this context, a carboxylate-based heterobimetallic lead–titanium complex was prepared from aqueous solution route, and the obtained complex was structurally characterized and used as a single-source precursor to synthesize $PbTiO_3$ nanopowder at low temperature calcinations.

Experimental

All the experiments were carried out in open air. All the chemicals were analytical reagents and were used without further purification. Nanopure-quality water was used throughout this study.

Preparation of the single-source precursor $[Pb(H_2O)_3]_2[Ti_2(O_2)_2O(NC_6H_6O_6)_2]\cdot 4H_2O$ (**1**)

The flowchart for synthesis of compound **1** and $PbTiO_3$ material is summarized in Scheme 1. To the suspension of H_3nta (9.57 g, 50 mmol) in 50 mL of deionized water was added slowly 17.2 mL $Ti(OC_4H_9)_4$ with stirring for 3 h. Hydrogen peroxide (10 mL, 30%) was added to the above mixture at room temperature with stirring, after which 18.97 g (50 mmol) of $Pb(CH_3COO)_2\cdot 3H_2O$ was added to the red solution slowly. Finally, the resulting solution was stirred for 0.5 h and yellow micro-crystals were precipitated. The yellow crystals were collected via filtration and washed three times with deionized water and once with ethanol. The product was dried in air to give compound **1** (51.59 g, 90% yield based on titanium). Elemental analysis for compound **1**: Found (Calcd. for $C_{12}H_{32}O_{27}N_2Pb_2Ti_2$): C, 12.40% (12.57%); H, 2.92% (2.81%); N, 2.10% (2.44%). IR (KBr, cm^{-1}): 3423_{vs}, 1629_{vs}, 1462_m, 1427_s, 1026_m, 925_m, 872_s, 770_s 739_s, 603_s, 538_m.

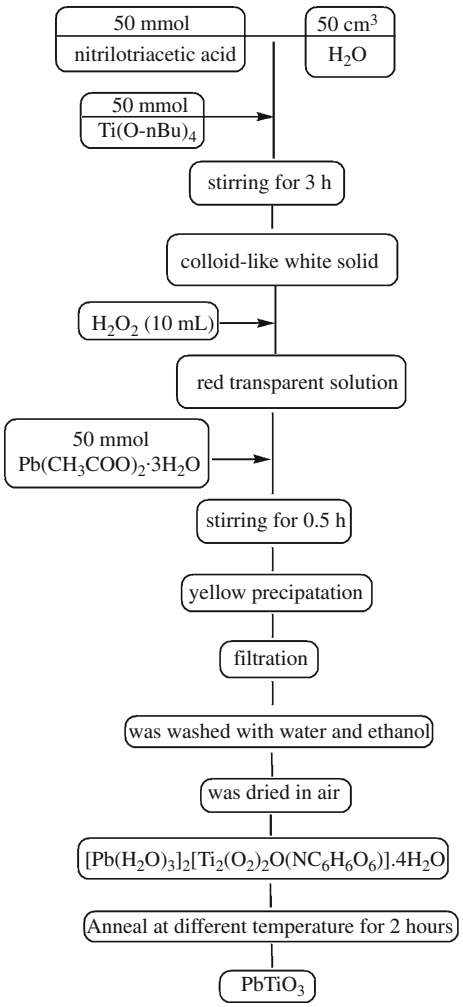

Scheme 1 Schematic representation of the major experiment steps involved in the preparation of complex **1** and $PbTiO_3$

Crystal of suitable quality for the subsequent X-ray single-crystal diffraction studies were obtained as transparent light yellow needle crystals from the diluted reaction solution. The crystals were mounted in capillary for X-ray analysis. Crystallographic data for **1**: crystal dimensions 0.25 × 0.20 × 0.15 mm, $C_{12}H_{32}O_{27}N_2Pb_2Ti_2$, Mr = 1146.58, triclinic, space group $P-1$, $a = 8.167$ (2) Å, $b = 9.763$ (2) Å, $c = 10.500$ (2) Å, $\alpha = 76.72$ (2), $\beta = 69.49$ (2), $\gamma = 67.38$ (2)°, $V = 719.4$ (2) $Å^3$, $Z = 1$, $D_c = 2.646$ g cm^{-3}, $\mu = 12.315$ mm^{-1}, 7,104 reflections were collected, of which 3,266 were unique ($R_{int} = 0.0566$). $R = 0.055$ and $wR_2 = 0.129$, GOF = 1.18 for 236 parameters. The intensity data were measured on a Rigaku R-AXIS SPIDER diffractometer with graphite-monochromated Mo Kα ($\lambda = 0.7107$ Å) at 297 (2) K. All calculations were performed using the SHELXL-97 program package [38]. The structure was solved by direct methods and refined by full-matrix least-squares methods.

All non-hydrogen atoms were refined anisotropically, hydrogen atoms were included but refined isotropically.

Physical measurements

Infrared spectrum was recorded (in the 4,000–400 cm^{-1}) as KBr disks on a Bruker 1600 FTIR spectrometer. Elemental analyses were performed using EA 1110 elemental analyzers. Thermogravimetric (TG) analysis was carried out using a Universal V4 4A Intruments with a heating rate 10 °C/min in flowing air. Powder diffraction patterns were obtained using a Rigaku D/Max-IIIA powder diffractmeter using Cu Kα radiation at 40 kV and 40 mA at a step of 0.020. The morphology of the calcined powder was observed by transmission electron microscope (TEM).

Results and discussion

X-ray structural analysis of compound **1**

Figure 1 presents the structure of the lead nitrilotriacetatoperoxotitanate compound determined from single-crystal X-ray diffraction data. This compound consists of two

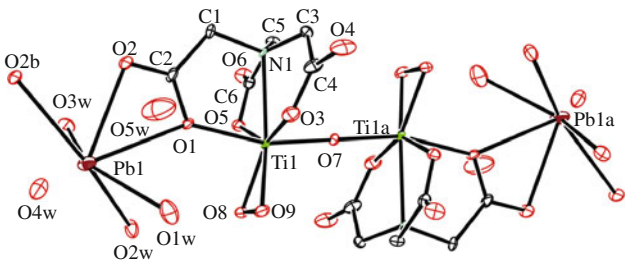

Fig. 1 ORTEP plot of $[Pb(H_2O)_3]_2[Ti(O_2)_2O(NC_6H_6O_6)_2]\cdot 4H_2O$ (**1**) at the 30% probability level, the hydrogen atoms were omitted for clarity. Selected bond distances (Å): Ti1–O1 2.080(7), Ti1–O3 2.085(9), Ti1–O5 2.073(8), Ti1–O7 1.814(2), Ti1–O8 1.907(8), Ti1–O9 1.887(8), Ti1–N1 2.283(8), O8–O9 1.477(9)

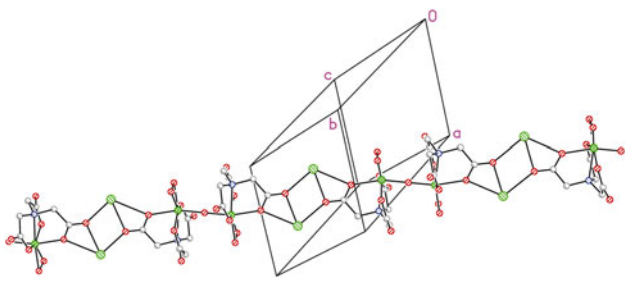

Fig. 2 The one-dimension MOF structure of complex **1**

peroxotitanate fragments interlinked through the bridging oxygen atom (O7). Each Ti atom in compound **1** is coordinated by three oxygen atoms and one nitrogen atom from a fully deprotonated nta^{3-} ligand, one bridging oxygen atom, and one peroxo group. The peroxo group binds to Ti(IV) in a side-on η^2-fashion, occupying two coordination sites in the equatorial plane. While the remaining three sites of the equatorial plane are occupied by two oxygen atoms (O3 and O5) and one nitrogen atom (N1) from the coordinated nta^{3-} ligand (The mean deviation from plane is 0.0605 Å). The apical positions are occupied with the two oxygen atoms (O1 and O7) from the carboxylate group of nta and bridging oxygen atom, respectively. As such, the coordination number around the Ti(IV) atom is seven, reflecting a distorted pentagonal-bipyramidal coordination environment. The binuclear $[Ti_2(O_2)_2O(nta)_2]^{4-}$ anionic structure of **1** is quite similar to that of the related main-group and transition metal-containing nitrilotriacetatoperoxotitanate complexes. The oxygen atoms (O1 and O2) of one of the carboxylate $-CO_2$ groups bind to the water-coordinated Pb atom, whose coordination polyhedron is a distorted octahedron. Adjacent asymmetric units are linked through O2b ($1 - x$, $2 - y$, $1 - z$) into a one dimensional metal organic frameworks (MOFs) (as shown in Fig. 2). The polymeric 1-D MOF is further linked by hydrogen bonds involving the water molecules and the carboxylate atoms, thus generating a 3D polymeric structure (as shown in Fig. 3). The Ti–$O_{carboxylate}$ bond distances in **1** [2.073(7)–2.085(7) Å] are similar to those found in related Ti(IV) peroxo complexes, like $[Ca(H_2O)_3]_2[Ti_2(O_2)_2O(nta)_2]\cdot 2H_2O$ [2.010(4)–2.111(4) Å] [36], $[Sr(H_2O)_4]_2[Ti_2(O_2)_2O(nta)_2]\cdot 2H_2O$ [2.072(4)–2.101(4) Å], $[Ba(H_2O)_5]_2[Ti_2(O_2)_2O(nta)_2]$ [2.066(4)–2.100(4) Å] [34], and $[M(H_2O)_5]_2[Ti_2(O_2)_2O(nta)_2]\cdot 7H_2O$ {M = Mn [2.066(2)–2.112(2) Å], Co [2.068(2)–2.109(2) Å], Ni [2.074(2)–2.114(2) Å], and Zn [2.069(1)–2.107(2) Å]} [37]. The O–O bond distance [1.477(13) Å] in the coordinated peroxo group is in normal range [39]. The Pb–O bond distances [2.515(9)–2.735(8) Å] are also in normal range [40].

Thermal decomposition process

Figure 4 illustrates the TG and DTA curves of compound **1** heat-treated in air using a heating rate of 10 °C/min in the temperature range 293–1,073 K. The TG of the as-prepared precursor shows marked mass losses with increasing temperature in three steps. The possible decomposition reactions are: (i) dehydration (323–473 K), (ii) decomposition of the nitriloacetate to a mixture of metal oxides or other intermediates (473–673 K), and (iii) decomposition of the intermediate phases to form $PbTiO_3$ (673–723 K). The first TG weight loss of approximately 6.1% in the temperature range 298–333 K with an endothermic peak at 325 K (Fig. 4) is mainly due to the departure of four lattice

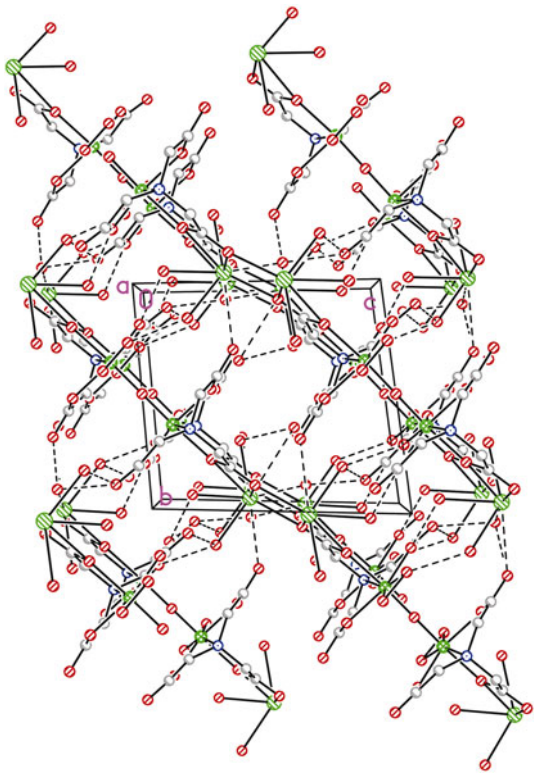

Fig. 3 The 3-dimension structure of complex **1** constructed by hydrogen bonds

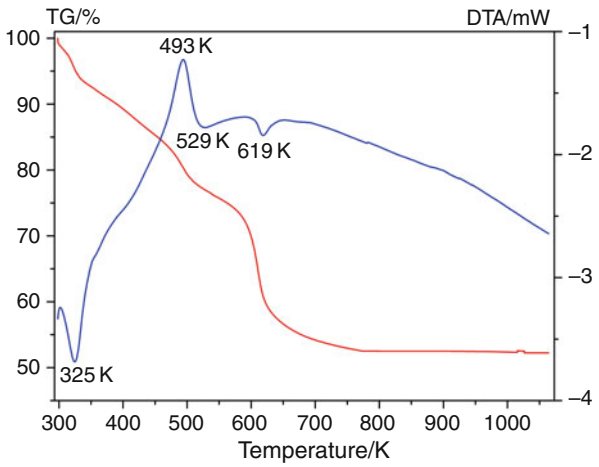

Fig. 4 The DTA–TG curves of complex **1**

(theoretical weight loss 6.3%) water molecules from complex **1**. The subsequent thermal decomposition of the $[Pb(H_2O)_3]_2[Ti_2(O_2)_2O(NC_6H_6O_6)_2]$, with a mass loss of 9.6% in the range 333–473 K, is contributed to the departure of six (theoretical weight loss 9.4%) coordination water molecules. Between 463 and 673 K, a strong weight loss and three main thermal events (an endothermic peak at 493 K, two exothermic peaks at 529 and 619 K, respectively) are visible. The weight loss is clearly attributed to the removal of organic ligands. In addition, a small mass loss (about 2.7%) is also visible between 673 and 773 K. No significant weight loss was observed for complex **1** when the temperature above 773 K. This result gives evidence for the absence of carbon and proves the stability of the obtained particles at high temperatures, especially regarding the commonly observed PbO loss through evaporation at temperatures above 973 K. The total mass loss observed from the TG curve is around 47.5%, which is in good agreement with the theoretical expected weight loss (47.2%) calculated from the pyrolysis of compound **1** to $PbTiO_3$.

Powder X-ray diffraction studies of the crystal phases of samples

Calcination treatments were performed to induce crystallization and the resulting XRD plots are shown in Fig. 5. Broad and very weak peaks showed up after the heat treatment at 623 K for 2 h, and the positions of which can be attributed to those for PbO and TiO_2 (not shown here). Of course at this temperature large amounts of amorphous material are still present, resulting in a high background and low diffraction intensities. The heat treatment of compound **1** at 450 °C for 2 h resulted in formation of tetragonal $PbTiO_3$ as a pure phase (as shown in Fig. 5), which indicated that a calcination temperature of 723 K was sufficient to obtain $PbTiO_3$. Powders annealed at 723, 773, 873, and 923 K could be indexed as tetragonal $PbTiO_3$ (JCPDS 06-0452). With increasing calcination

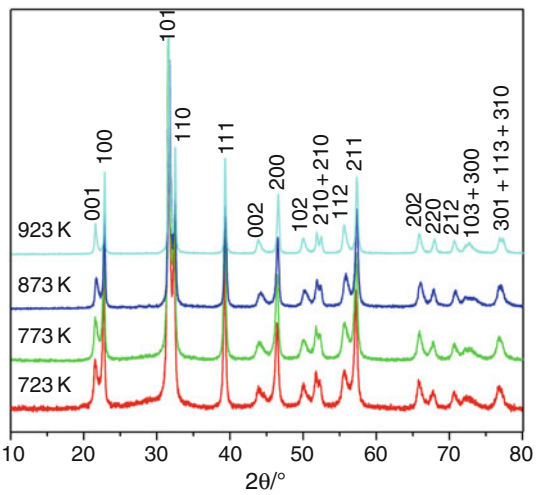

Fig. 5 X-ray powder diffraction patterns of the samples obtained from complex **1** at different temperature, with holding in air for 2 h

temperature, the peak intensities to $PbTiO_3$ became stronger and all reflections could be assigned to $PbTiO_3$. There was no evidence for phase separation. The above results are in good agreement with the TG–DTA analysis result. The full-width at half-maximum (FWHM) of the (00l) reflections is larger than the FWHM of the (100) reflections. Similar results have been reported by Moon et al. [41] and selbach et al. [42] for $PbTiO_3$ prepared by the hydrothermal method and sol–gel route, respectively. They proposed that the peak broadening due to strain in the c-axis direction is much higher than in the a-axis direction, while the domain sizes for both directions are similar.

FTIR spectrometry

To trace some possibly existed organic species and the initial formation of Ti–O–Ti bonds in the calcined samples, the changes of FTIR spectra for complex 1 and the as-prepared samples at different calcinations temperatures were shown in Fig. 6. The band at $\sim$3,400 cm^{-1} was attributed to the O–H stretching vibrations of water molecules in compound **1**. The bands at $\sim$1,630 and $\sim$1,430 cm^{-1} are assigned to the unantisymmetric and symmetric stretching vibrations of carboxylate, respectively. The frequencies of the bands of the antisymmetric and symmetric stretching vibrations are shifted to lower values compared to the corresponding vibrations in free H_3nta, thus indicating a change in the coordination status of the carboxylates in the H_3nta ligand. The O–O vibration of the peroxo groups in **1** was at 872 cm^{-1}. There is also a band around 603 cm^{-1}, which has been attributed to the presence of $V_{as}(Ti–(O_2))$ vibrations. The corresponding frequency for the $V_s(Ti–(O_2))$ vibrations was observed around 538 cm^{-1}. There is no obvious difference between complex **1** and the sample of complex **1** which was calcined at 373 K, except the weaker peak around 3,400 cm^{-1}, which is probably attributed to the crystallized water molecules which were lost in the complex **1**. The peaks at 872 and 730 cm^{-1} were disappeared when the calcined temperature is increased to 473 K. This result indicated that the peroxo groups in complex **1** have been decomposed. Simultaneously, the peaks corresponding to the CO_3^{2-} group at about 1436, 1059, 856, and 693 cm^{-1} have been observed, although the peaks were very weak. In addition, the intensity of the vibrations at 1,630 and 1,420 cm^{-1} decreased. These results suggested that the nta^{3-} ligands began to decompose and some carbonate was formed in this temperature. Some organic residues were traced between 1,650 and 1,100 cm^{-1} for the sample calcined at 623 K, and the peaks for CO_3^{2-} disappear, indicating that the intermediates in this temperature did not contain carbonate. The reason for this is that $PbCO_3$ decomposes at this temperature. The peaks around 3400, 1600, and 1420 cm^{-1} for the sample became weaker and weaker with the raise of temperature and did not disappear completely, indicating the escape of the organic residues and the existence of some adsorbed water on the surface of particles. In addition, a very broad absorption band from 500 to 700 cm^{-1} was observed, which was due to the bending vibration of Ti–O–Ti bonds. With increasing calcination temperature, the Ti–O–Ti absorption peaks became stronger.

Based on the above results of TG, XRD, and IR spectra, a possible thermal decomposition steps of complex **1** are proposed (as shown in Scheme 2).

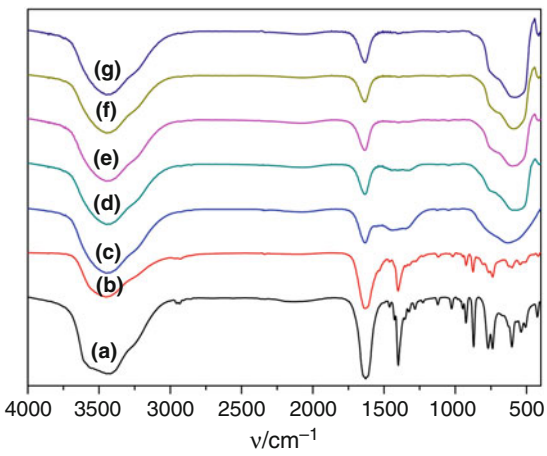

Fig. 6 FTIR spectra of the samples obtained from complex **1** at different temperature, with holding in air for 2 h, **a** complex **1**, **b** 373 K, **c** 473 K, **d** 523 K, **e** 623 K, **f** 773 K, and **g** 873 K

Morphology observation and BET measurement

Figure 7 shows the transmission electron images of the $PbTiO_3$ nanoparticles obtained from pyrolysis complex **1** at 773 K for 2 h. It was found that $PbTiO_3$ powders only consisted of the nano-scale crystallites with the crystalline size of 60–100 nm and a tetragonal flake-like shape. Figure 8 shows the N_2 adsorpotion/desorpotion isotherm and the corresponding pore size distribution of the $PbTiO_3$ samples. The measurement shows that the BJH (Barrett–Joyner–Halenda) desorpotion gives a main pore size distribution ranging from 40–70 nm to 90–110 nm with average pore size of 47.8 nm, which can be attributed to the interparticle pores. The pores with wider pore size distribution can be attributed to the irregular sizes of the samples. The BET surface area of the nanocrystalline $PbTiO_3$ powders was measured to be 5.6 m^2/g at 773 K.

Scheme 2 Schematic representation of the major steps involved in the thermal decomposition of complex **1**

$$[Pb(H_2O)_3]_2[Ti_2(O_2)_2O(NC_6H_6O_6)_2]\cdot 4H_2O \xrightarrow{298 \text{ to } 333\ K} [Pb(H_2O)_3]_2[Ti_2(O_2)_2O(NC_6H_6O_6)_2]$$

$$[Pb(H_2O)_3]_2[Ti_2(O_2)_2O(NC_6H_6O_6)_2] \xrightarrow{333 \text{ to } 473\ K} PbCO_3 + [Ti_2O(NC_6H_6O_6)_2]$$

$$PbCO_3 + [Ti_2O(NC_6H_6O_6)_2] \xrightarrow{473 \text{ to } 623\ K} PbO + TiO_2$$

$$PbO + TiO_2 \xrightarrow{623 \text{ to } 723\ K} PbTiO_3$$

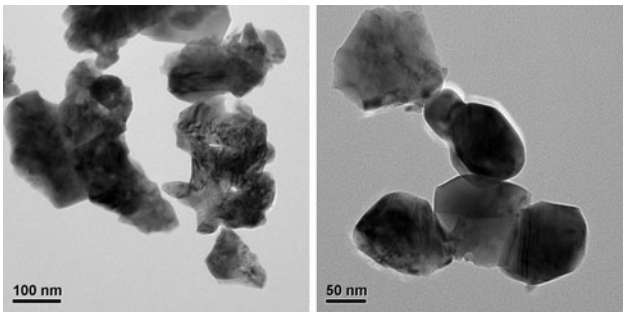

Fig. 7 TEM image of $PbTiO_3$ from the thermal decomposition of complex **1** at 773 K

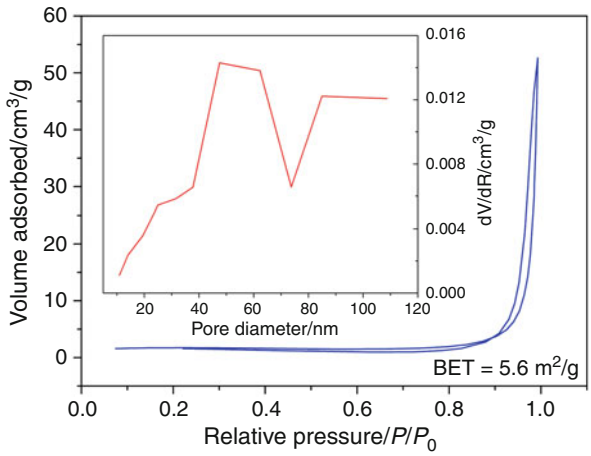

Fig. 8 N_2 adsorption–desorption isotherms and BJH pore size distribution curves of the $PbTiO_3$ obtained from the thermal decomposition of complex **1** at 773 K

Conclusions

In summary, a general and simple route has been developed for the preparation of a new heterobimetallic lead nitrilotriacetatoperoxotitanate compound. This structurally characterized compound gives rise to phase-pure nanoparticles of $PbTiO_3$ powders with a crystalline size varying from 60 to 100 nm when heated at 773 K. The compound is highly stable toward hydrolysis and, therefore, has potential applications in cheap and convenient syntheses of a variety of $PbTiO_3$-based materials for industrially important products.

Supplementary material

Crystallographic data for the structural analysis have been deposited with the Cambridge Crystallographic Data Centre, CCDC No. 783100 for compound **1**. Copies of this information are may be obtained free of charge from The Director, CCDC, 12 Union Road, Cambridge, CB2 1EZ, UK (fax: +44-1223-336033; email: deposit@ccdc.cam.ac.uk or www: http://www.ccdc.cam.ac.uk).

Acknowledgements We thank "The Fundamental Research Funds for the Central Universities, SCUT (No. 2009ZM0313)". We also thank "The National Science Foundation of China (No. B5080320)" and the "SRP" of South China University of Technology.

References

1. Jaffe WJ, Cook R, Jaffe H. Piezoelectric ceramics. New York: Academic Press; 1971.
2. Lines ME, Glass AM. Principles and applications of ferroelectrics and related materials. Oxford, UK: Oxford University Press; 2001.
3. Scott JF. Applications of modern ferroelectrics. Science. 2007;315:954–9.
4. Yang Y, Wang XH, Sun CK, Li LT. Photoluminescence of high-aspect-ratio $PbTiO_3$ nanotube arrays. J Am Ceram Soc. 2008;91:3820–2.
5. Garnweitner G, Hentschel J, Antonietti M, Niederberger M. Nonaqueous synthesis of amorphous powder precursors for nanocrystalline $PbTiO_3$, Pb(Zr, Ti)O_3, and $PbZrO_3$. Chem Mater. 2005;17:4594–9.
6. Ishikawa K, Yoshikawa K, Okada N. Size effect on the ferroelectric phase transition in $PbTiO_3$ ultrafine particles. Phys Rev B. 1998;37:5852–5.
7. Zhong WL, Wang YG, Zhang PL, Wu BD. Phenomenological study of the size effect on phase transitions in ferroelectric particles. Phys Rev B. 1994;50:698–703.
8. Liu C, Zou BS, Rondinone AJ, Zhang ZJ. Sol-gel synthesis of free-standing ferroelectric lead zirconate titanate nanoparticles. J Am Chem Soc. 2001;123:4344–5.
9. Ren ZH, Xu G, Liu Y, Wei X, Zhu YH, Zhang XB, Lv GL, Wang YW, Zeng YW, Du PY, Weng WJ, Shen G, Jiang JZ, Han GR. $PbTiO_3$ nanofibers with edge-shared TiO_6 octahedra. J Am Chem Soc. 2010;132:5572–3.
10. Teff DJ, Caulton KG. Hydrolytic synthesis of lead oxo isopropoxides and their reaction with $M((OPr)Pr^i)_4$ (M = Ti, Zr): comparisons and contrasts. Inorg Chem. 1998;37:2554–62.
11. Veith M. Molecular precursors for (nano) materials—a one step strategy. J Chem Soc Dalton Trans. 2002;32:2405–12.
12. Hubert-Pfalzgraf LG. Some trends in the design of homo- and heterometallic molecular precursors of high-tech oxides. Inorg Chem Commun. 2003;6:102–20.

13. Kessler VG. Molecular structure design and synthetic approaches to the heterometallic alkoxide complexes (soft chemistry approach to inorganic materials by the eyes of a crystallographer). Chem Commun. 2003;39:1213–22.
14. Veith M, Haas M, Huch V. Single source precursor approach for the sol–gel synthesis of nanocrystalline $ZnFe_2O_4$ and zinc-iron oxide composites. Chem Mater. 2005;17:95–101.
15. Li JG, Yang X, Ishigaki T. Urea coordinated titanium trichloride $Ti^{III}[OC(NH)_2]_6Cl_3$: a single molecular precursor yielding highly visible light responsive TiO_2 nanocrystallites. J Phys Chem B. 2006;110:14611–8.
16. Hamid M, Tahir AA, Mazhar M, Zeller M, Hunter AD. Heterobimetallic molecular cages for the deposition of Cu/Ti and Cu/Zn mixed-metal oxides. Inorg Chem. 2007;46:4120–7.
17. Malghe YS, Dharwadkar SR. $LaCrO_3$ powder from lanthanum trisoxalatochromate(III) (LTCR) precursor-Microwave aided synthesis and thermal characterization. J Therm Anal Calorim. 2008;95:915–8.
18. Thomas P, Dwarakanath K, Varma KBR, Kutty TRN. Synthesis of nanoparticles of the giant dielectric material, $CaCu_3Ti_4O_{12}$ from a precursor route. J Therm Anal Calorim. 2009;95:267–72.
19. Tahir AA, Mazhar M, Hamid M, Wijayantha KGU, Molloy KC. Photooxidation of water by $NiTiO_3$ deposited from single source precursor $[Ni_2Ti_2(OEt)_2(\mu\text{-}OEt)_6(acac)_4]$ by AACVD. Dalton Trans. 2009;38:3674–80.
20. Gonsalves LR, Verenkar VMS, Mojumdar SC. Preparation and characterization of $Co_{0.5}Zn_{0.5}Fe_2(C_4H_2O_4)_3{\cdot}6N_2H_4$. J Therm Anal Calorim. 2009;96:53–7.
21. Gawas UB, Mojumdar SC, Verenkar VMS. Synthesis, characterization, infrared studies, and thermal analysis of $Mn_{0.6}Zn_{0.4}(C_4H_2O_4)_3{\cdot}6N_2H_4$ and its decomposition product $Mn_{0.6}Zn_{0.4}Fe_2O_4$. J Therm Anal Calorim. 2010;100:867–71.
22. Thurston J, Whitmire KH. Heterobimetal lic bismuth-transition metal salicylate complexes as molecular precursors for ferroelectric materials. Synthesis and structure of $Bi_2M_2(sal)_4(Hsal)_4(OR)_4$ (M = Nb, Ta; R = CH_2CH_3, $CH(CH_3)_2$, $Bi_2Ti_3(sal)_8(Hsal)_2$, and $Bi_2Ti_4((OPr)Pr^i)(sal)_{10}(Hsal)$ (sal = $O_2CC_6H_4$–2–O; Hsal = $O_2CC_6H_4$–2–OH). Inorg Chem. 2002;41:4194–205.
23. Zhang HT, Yang JH, Shpanchenko RV, Abakumov AM, Hadermann J, Clérac R, Dikarev EV. New class of single-source precursors for the synthesis of main group-transition metal oxides: heterobimetallic Pb–Mn β-diketonates. Inorg Chem. 2009;48:8480–8.
24. Chae HK, Payne DA, Xu Z, Ma L. Molecular structure of a new lead titanium bimetallic alkoxide complex, $[PbTi_2(\mu_4\text{-}O)(OOCCH_3)(OCH_2CH_3)]_2$: evolution of structure on heat treatment and the formation of thin-layer dielectrics. Chem Mater. 1994;6:1589–92.
25. Daniele S, Papiernik R, Hubert-Pfalzgraf LG, Jagner S, Håkansson M. Single-source precursors of lead titanate: synthesis, molecular structure and reactivity of $Pb_2Ti_2(\mu_4\text{-}O)$ $(\mu_3\text{-}O\text{-}i\text{-}Pr)_2(\mu\text{-}O\text{-}^iPr)(O\text{-}i\text{-}Pr)_4$. Inorg Chem. 1995;34:628–32.
26. Hubert-Pfalzgraf LG, Daniele S, Papiernik R, Massiani MC, Septe B, Vaissermann J, Daran JC. Solution routes to lead titanate: synthesis, molecular structure and reactivity of the Pb–Ti and Pb–Zr species formed between various lead oxide precursors and titanium or zirconium alkoxides. Molecular structure of $Pb_2Ti_2(\mu_4\text{-}O)(OAc)_2(OPri)_8$ and of $PbZr_3$ $(\mu_4\text{-}O)(OAc)_2(OPri)_{10}$. J Mater Chem. 1997;7:753–62.
27. Boulmaâz S, Papiernik R, Hubert-Pfalzgraf LG, Septe B, Vaissermann J. J Mater Chem. 1997;7:2053.
28. Mishra S, Daniele S, Hubert-Pfalzgraf LG. Metal 2-ethylhexanoates and related compounds as useful precursors in materials science. Chem Soc Rev. 2007;37:1770–87. and reference therein.
29. Zhou ZH, Deng YF, Jiang YQ, Wan HL, Ng SW. The first structural examples of tricitratotitanate $[Ti(H2cit)_3]^{2-}$ dianions. Dalton Trans. 2003;33:2636–8.
30. Deng YF, Zhou ZH, Wan HL, Tsai KR. Ammonium barium citrato peroxotitanate(IV) $Ba_2(NH_4)_2[Ti_4(O_2)_4(Hcit)_2(cit)_2]{\cdot}10H_2O$: a molecular precursor of stoichiometric $BaTi_2O_5$. Inorg Chem Commun. 2004;7:169–72.
31. Deng YF, Zhou ZH, Wan HL. pH-Dependent isolations and spectroscopic, structural, and thermal studies of titanium citrate complexes. Inorg Chem. 2004;43:6266–73.
32. Deng YF, Zhang HL, Hong QM, Weng WZ, Wan HL, Zhou ZH. Titanium-based mixed oxides from a series of titanium(IV) citrate complexes. J Solid State Chem. 2007;180:3152–9.
33. Deng YF, Zhou ZH. A stable water-soluble molecular precursor for the preparation of stoichiometric strontium titanate. Inorg Chem Commun. 2008;11:1064–6.
34. Zhou ZH, Hong QM, Deng YF. Pure Ti-based mixed oxides prepared from the thermal decompositions of molecular precursors of peroxo complexes coordinated with tris(hydroxycarbonylmethyl) amine trivalent anion Titanate(IV). Acta Chim Sinica. 2004;62:2379–85.
35. Deng YF, Tang SD, Lao LQ, Zhan SZ. Synthesis of magnesium titanate nanocrystallites from a cheap and water-soluble single source precursor. Inorg Chim Acta. 2010;363:827–9.
36. Deng YF, Tang SD, Wu SP. Synthesis of calcium titanate from $[Ca(H_2O)_3]_2[Ti_2(O_2)_2O(NC_6H_6O_6)_2]{\cdot}2H_2O$ as a cheap single-source precursor. Solid State Sci. 2010;12:339–44.
37. Deng YF, Lv QY, Wu SP, Zhan SZ. Heterobimetallic peroxotitanium(IV) nitrilotriacetate complexes as single source precursors for preparation of $MTiO_3$ (M = Co, Ni and Zn). Dalton Trans. 2010;39:2497–503.
38. Sheldrick GM. Schelxl-97, Program for refinement of crystal structure. Göttingen, Germany: University of Göttingen; 1997.
39. Kakihana M, Tada M, Shiro M, Petrykin V, Osda M, Nakamura Y. Structure and stability of water soluble $(NH4)_8[Ti_4(C_6H_4O_7)_4(O_2)_4]{\cdot}8H_2O$. Inorg Chem. 2001;40:891–4.
40. Kourgiantakis M, Matzapetakis M, Raptopoulou CP, Terzis A, Salifoglou A. Lead-citrate chemistry. Synthesis, spectroscopic and structural studies of a novel lead(II)-citrate aqueous complex. Inorg Chim Acta. 2000;297:134–8.
41. Moon J, Li T, Randall CA, Adair JH. Low temperature synthesis of lead titanate by a hydrothermal method. J Mater Res. 1997;12:189–97.
42. Selbach SM, Wang GZ, Einarsrud MA, Grande T. Decomposition and crystallization of a sol–gel-derived $PbTiO_3$ precursor. J Am Ceram Soc. 2007;90:2649–52.